Interaction between the Atlantic meridional and Niño modes

Gregory R. Foltz[1] and Michael J. McPhaden[2]

Received 14 May 2010; revised 23 July 2010; accepted 5 August 2010; published 22 September 2010.

[1] Interaction between the tropical Atlantic meridional and Niño modes is investigated using observations and a quasi-analytical linear equatorial wave model. It is found that equatorial zonal wind stress anomalies associated with the boreal spring meridional mode generate eastward propagating equatorial Kelvin waves in the central and eastern Atlantic Ocean, where variability associated with the Niño mode is strongest. These same wind stress anomalies force westward propagating equatorial Rossby waves that reflect at the western boundary into eastward propagating Kelvin waves during boreal spring and summer. The boundary-generated Kelvin waves are of the opposite sign to those directly forced by the winds earlier in the spring, so they tend to damp the Niño mode during boreal summer. The interaction between the boreal spring meridional mode and the summer Niño is therefore mediated by directly wind-forced equatorial Kelvin waves and the delayed negative feedback from western boundary reflections of wind-forced Rossby waves.
Citation: Foltz, G. R., and M. J. McPhaden (2010), Interaction between the Atlantic meridional and Niño modes, *Geophys. Res. Lett.*, *37*, L18604, doi:10.1029/2010GL044001.

1. Introduction

[2] Climate variability in the tropical Atlantic consists of two distinct modes: the Niño mode, which is the Atlantic counterpart to the Pacific El Niño Southern Oscillation (ENSO), and the meridional mode, which does not have a strong analog in the Pacific. SST anomalies associated with the Niño mode are driven mainly by ocean dynamics, reflected in the strong positive correlation between sea level and SST in the eastern equatorial Atlantic [*Carton and Huang*, 1994; *Hu and Huang*, 2006] (Figure 1b). Positive feedback between SSTs, zonal winds, and thermocline depth (i.e., Bjerknes feedback) tends to sustain and prolong the Niño mode in the boreal spring and summer [*Chang et al.*, 2000; *Keenlyside and Latif*, 2007]. The Atlantic meridional mode (AMM), on the other hand, is characterized by an anomalous meridional gradient of SST centered near the latitude of the thermal equator (~5°N). Anomalous surface winds are directed toward the warmer hemisphere, resulting in a meridional displacement of the rain-producing intertropical convergence zone (ITCZ) [*Nobre and Shukla*, 1996] (Figure 1a). Wind-induced evaporation and positive wind-evaporation-SST feedback appear to be important drivers of the AMM [*Carton et al.*, 1996; *Chang et al.*, 2000].

[3] The separation of tropical Atlantic interannual variability into the AMM and Niño mode is based on two physical distinctions. First, different mechanisms are responsible for driving each mode: ocean dynamics are important for the Niño mode, whereas the AMM is thought to be primarily driven by air-sea heat fluxes and therefore thermodynamic in nature. Second, the modes have different seasonalities: the Niño mode is strongest in boreal summer, whereas the AMM peaks in boreal spring. Despite these differences, the spatial patterns of eastern equatorial SST and sea level associated with each mode are strikingly similar (Figure 1), suggesting the possibility of a dynamical connection.

[4] A possible mechanism linking the modes was proposed by *Servain et al.* [1999]. They suggested that a positive AMM in boreal spring (i.e., anomalously warm SSTs to the north of the ITCZ relative to the south) may induce easterly anomalous winds on and south of the equator, generating cold equatorial SST anomalies in boreal summer through a combination of anomalous wind-induced evaporation and upwelling. Tendencies of opposite sign would apply to negative AMM periods. However, the Niño mode in boreal summer is only weakly correlated with the AMM of the preceding boreal spring (correlation of −0.3 for 1982–2009 between the meridional mode in April and the Niño mode in July with a 95% significance level is of 0.4). In this study we expand on the work of *Servain et al.* [1999] to provide a more complete description of how the meridional and Niño modes interact. It is shown that equatorial Rossby waves generated by AMM-induced wind stress anomalies provide a delayed negative feedback on the development of the Niño mode the following summer. This delayed negative feedback provides a possible explanation for the observed weak correlation between the boreal spring meridional mode and the boreal summer Niño.

2. Data and Model

[5] A combination of observational and atmospheric reanalysis data sets and a linear equatorial wave model are used in this study. SST from a monthly combined satellite/in situ SST product is available on a 1° × 1° grid for Dec 1981–present [*Reynolds et al.*, 2002]. We use the merged satellite sea level anomaly product from Archiving, Validation and Interpretation of Satellite Oceanographic data (AVISO). Sea level anomalies with respect to the 1993–1999 mean are generated a 1° × 1° grid. Weekly averages are available from October 1992 through June 2006 and daily averages from July 2006 to the present. We also use daily surface wind velocity from the NCEP/NCAR reanal-

[1]Joint Institute for the Study of the Atmosphere and Ocean, University of Washington, Seattle, Washington, USA.
[2]Pacific Marine Environmental Laboratory, NOAA, Seattle, Washington, USA.

0094-8276/10/2010GL044001

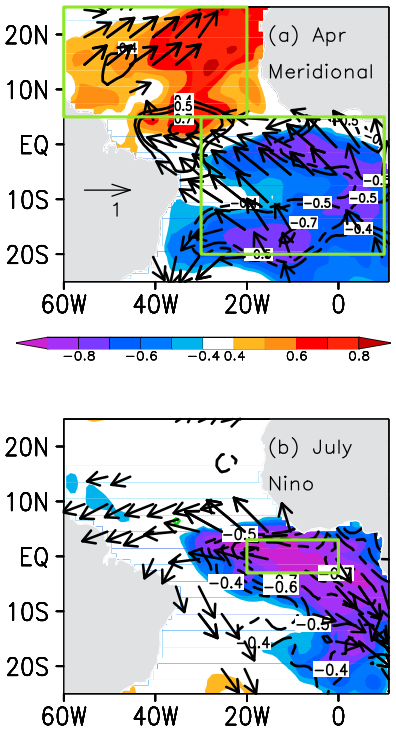

Figure 1. (a) Correlation of SST (shaded), wind stress (vectors), and sea level (contours) anomalies in April with the April Atlantic meridional mode (AMM) index (SST averaged 5°N–28°N, 20°W–60°W minus 20°S–5°N, 30°W–10°E) for 1993–2009. (b) Same as Figure 1a except correlations between July SST, wind stress, and sea level with the July Atl-3 index (SST averaged 0°–20°W, 3°S–3°N). Boxes in Figures 1a and 1b show the regions used to define the AMM index and the Atl-3 index, respectively. Anomalies are with respect to the 1993–2008 monthly mean seasonal cycle after removal of the linear trend. Correlations are shown only where significant at 90% based on a 1000-sample permutation test.

ysis for 1948–present on a 2° × 2° grid [*Kalnay et al.*, 1996]. All data sets are averaged to monthly means. We restrict the analysis to the period Jan 1993–Oct 2009, when all data sets are available. Anomalies are calculated with respect to the monthly mean climatology for the period 1993–2008.

[6] The linear wave model used in this study is described in detail by *Yu and McPhaden* [1999]. The model is continuously stratified, and the longwave approximation has been made to filter out all waves except Kelvin and long Rossby waves. The model uses the method of characteristics to solve for wind-forced Kelvin and Rossby waves. Boundary-generated waves are determined analytically by requiring zero zonal net mass flux at the western boundary and zero zonal velocity at the eastern boundary. Vertical modes are calculated using the annual mean density stratification from World Ocean Atlas 2005 (WOA05) temperature and salinity from the surface to 3000 m averaged between 5°S and 5°N. We have retained the first 10 baroclinic modes and 15 meridional modes (Kelvin plus first 14 Rossby). Phase speeds for the first and second baroclinic mode Kelvin waves are 2.3 and 1.4 m s^{-1}, respectively, and for the first and second baroclinic mode Rossby waves the phase speeds are 0.8 and 0.5 m s^{-1}, respectively. These values are in agreement with previous studies in the equatorial Atlantic [e.g., *Illig et al.*, 2004]. Results are not sensitive to the region used to calculate the mean density profile.

[7] The model is unbounded in the meridional direction, and the zonal domain is 8°E–50°W, with meridional walls at the eastern and western boundaries. The reflection efficiency at the western boundary is set to 85% following *McCalpin* [1987]. The reflection efficiency at the eastern boundary is set to 65% following *Illig et al.* [2004]. Despite the idealization of the eastern and western boundaries, the model reproduces observed variability of sea level in the equatorial Atlantic reasonably well (Figures S1–S3 of the auxiliary material).[1] The model also compares very well with a linear wind-driven numerical model that has more realistic coastal boundaries (Figures S4 and S5).

[8] The grid sizes are Δt = 12 hr and Δx = 2°. The damping coefficient is A/c_n^2, where c_n is the vertical mode number. The parameter A is chosen so that the damping coefficient for the first vertical mode is (12 months)$^{-1}$. We have run the model with different boundary reflection efficiencies (ranging from 50% to 100%) and damping coefficients (A_1 ranging from 6 months to 24 months) and found that the basic results in this study are unchanged. The model is forced with daily NCEP/NCAR reanalysis zonal wind stress during January 1992–December 2009. Output from 1993–2009 is used in this study to avoid transients associated with the first year of model spin up. Wind stress is calculated using a constant drag coefficient of 2×10^{-3} and an air density of 1.29 kg m^{-3}. To test the sensitivity of our results to the choice of wind forcing, we ran the model with QuikSCAT winds for the period 2000–2009 and analyzed the output from 2001–2009. Though some of the features in the QuikSCAT run were sharpened, overall the results were similar to the NCEP run for the overlapping period (2001–2009). Our preference therefore was to use the NCEP-forced run because its longer duration coincides with the full altimeter record.

3. Results

[9] In this section we investigate the interaction between the meridional and Niño modes, focusing on the role of equatorial waves. Previous studies have shown that equatorial Kelvin waves play an important role in the evolution of SST anomalies in the eastern equatorial Atlantic. Easterly (westerly) wind anomalies in the western basin generate anomalous upwelling (downwelling) that propagates eastward along the equator as a Kelvin wave, reaching the eastern boundary 1–2 months later [*Servain et al.*, 1982]. The SST anomalies associated with the Kelvin wave are strongest in the eastern basin, where the mean thermocline is shallowest [*Carton and Huang*, 1994; *Hormann and Brandt*, 2009]. Consistent with this interpretation and the results of *Servain et al.* [1999], we find that an anomalously positive (negative) meridional SST gradient in boreal spring is associated with easterly (westerly) equatorial wind anomalies and an anomalous shoaling (deepening) of the thermocline in the eastern equatorial Atlantic (Figure 1a).

[1] Auxiliary materials are available in the HTML. doi:10.1029/2010GL044001.

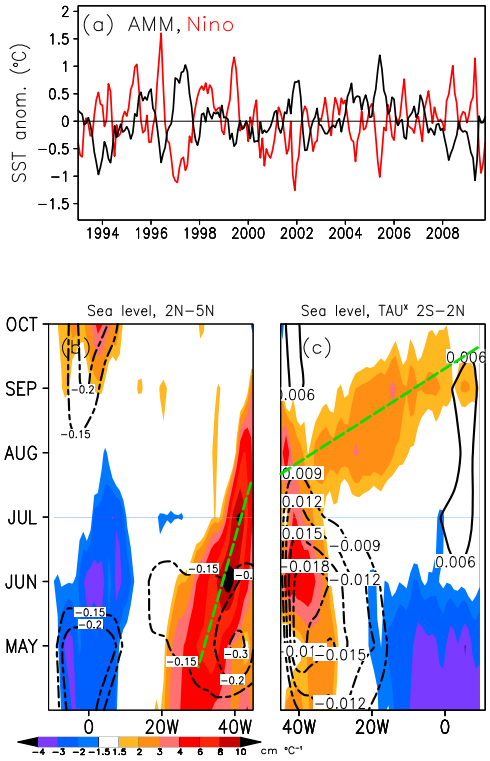

Figure 2. (a) Monthly AMM (black) and Niño (red) indexes for 1993–2009 (see Figure 1 for definition of indexes). (b) Lagged regression coefficients of anomalous sea level (shaded) and Ekman pumping velocity (contours, negative downward in units of m day^{-1} °C^{-1}) averaged in the 2°N–5°N band with the April AMM index. The longitude axis has been reversed to show reflection at the western boundary. (c) Same as Figure 2b but averaged in 2°S–2°N. Contours are regression coefficients of zonal wind stress onto the April AMM index, averaged in the same latitude band, in units of N m^{-2}(°C)$^{-1}$. Regressions are shown only where significant at 90%. Dashed green line in Figure 2b corresponds to April–July average westward phase speed of observed sea level anomalies as determined from correlation analysis. The phase speed does not correspond to any individual theoretical free Rossby wave phase speed because more than one meridional mode Rossby wave is involved and the waves are forced rather than free. Dashed green line in Figure 2c is the theoretical second baroclinic mode Kelvin wave phase speed.

[10] The same pattern of anomalous wind stress that generates sea level anomalies in the eastern basin gives rise to sea level anomalies of the opposite sign centered near 4°N in the western basin (Figure 1a). The sea level anomalies in the west appear to be driven by anomalous wind stress curl and associated Ekman pumping, consistent with previous results [*Zebiak*, 1993; *Carton and Huang*, 1994]. To investigate the potential impact of the AMM-generated sea level and wind anomalies on the Atlantic Niño mode, we perform lagged linear correlation and regression analyses onto the AMM index. The analysis is centered on April, the month with the strongest zonal wind stress, wind stress curl, and sea level anomalies in the western equatorial Atlantic (Figure 1a).

[11] The sea level anomalies generated by the AMM in April persist through June in the central and western basin between 20°W–45°W (Figure 2b). There are sea level anomalies of the opposite sign in the eastern equatorial Atlantic (20°W–10°E) during April–June, consistent with the sign of the equatorial wind stress anomalies and equatorial wave theory (Figure 2c). During June–August there is a relaxation of the anomalous zonal wind stress and wind stress curl between 20°W–45°W. The sea level anomalies in the western basin propagate westward, presumably as a packet of Rossby waves, to the coast of South America (Figure 2b). During July–September there is distinct eastward propagation of sea level anomalies from the western boundary to ~10°W (Figure 2c), suggesting that the westward propagating sea level anomaly has reflected into an equatorial Kelvin wave train. The speed of the eastward propagation is 1.3 m s^{-1}, corresponding well to the 1.4 m s^{-1} phase speed of the second baroclinic mode Kelvin wave. Zonal wind anomalies along the equator are weak during July–September, when the eastward propagation is most pronounced. As a result, it is unlikely that the eastward propagation is due directly wind-forced equatorial Kelvin waves.

[12] In order to investigate the role of linear equatorial waves in forcing the observed sea level anomalies, we turn to the results of the linear wave model. For consistency with the observational analysis, we perform lagged correlation and regression analyses between modeled sea level and the observed AMM index, centered on the month of April. The model reproduces well the sea level anomalies associated with the AMM (Figures 3a and 3b). Sea level anomalies generated in the central basin during April propagate westward and reach the western boundary during May–August. There is evidence of eastward propagation along the equator during August–September, though the signal is weaker compared to observations. The second baroclinic mode is the most energetic in the model solution, explaining 50–60% of interannual sea level variability in the equatorial band compared to 20–40% for the first baroclinic mode. These results agree with previous modeling studies [e.g., *Illig et al.*, 2004] and are supported by the observations (Figure 2c).

[13] One of the main advantages of using our quasi-analytical linear wave model is that the relative importance of wind-forced and boundary-reflected waves can easily be diagnosed. The sea level anomalies in the western basin at 4°N are associated mainly with wind-forced first and second meridional mode equatorial Rossby waves. Only the odd number meridional mode Rossby waves will reflect into Kelvin waves at the western boundary in our model since even meridional mode Rossby waves are associated with no net zonal mass transport integrated across latitude. Thus, the eastward-propagating sea level anomaly signal along the equator during August–September results mainly from the reflection of first meridional mode equatorial Rossby waves at the western boundary into eastward-propagating equatorial Kelvin waves of the same sign (Figures 3c and 3d). The reflected Kelvin waves are strongest in June–August, corresponding to the period with the strongest wind-forced

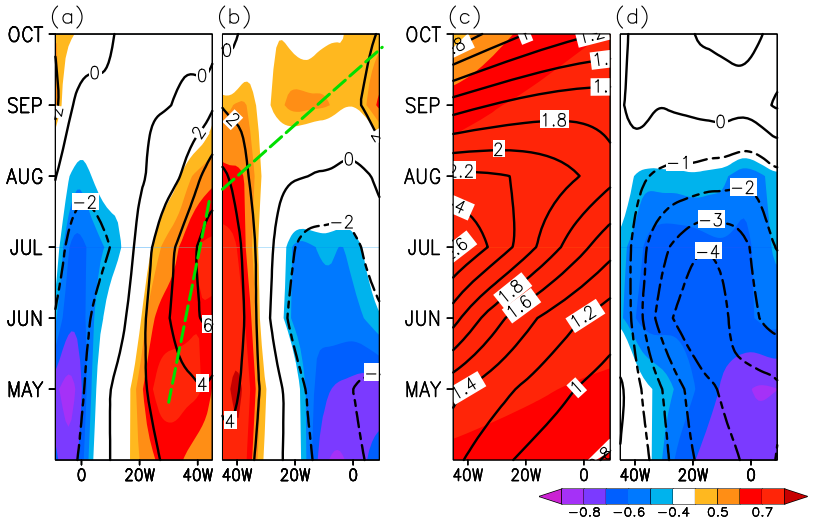

Figure 3. (a) Lagged correlation (shaded) and regression (contours) coefficients of anomalous sea level from the model, averaged in the 2°N–5°N band, with the observed April AMM index. The longitude axis has been reversed to show reflection at the western boundary. (b) Same as Figure 3a but averaged in 2°S–2°N. (c) Same as Figure 3b except correlations and regressions are with the reflected equatorial Kelvin waves. (d) Same as Figure 3c except for wind-forced equatorial Kelvin wave signal. Dashed green line in Figure 3a corresponds to the observed westward propagation of wind-forced Rossby waves as in Figure 2b. Dashed green line in Figure 3b is the theoretical second baroclinic mode Kelvin wave phase speed. Correlations are shown only where significant at the 90% level. Units of regression coefficients are cm $°C^{-1}$.

equatorial Rossby wave signal at 4°N. During May–July there is also a strong wind-forced Kelvin wave on the equator that is opposite in sign and stronger in amplitude than the reflected Kelvin wave based on the strength of the linear regression onto the AMM index (Figures 3c and 3d). The wind-forced Kelvin wave appears to propagate westward, but this is an artifact resulting from the westward migration of the easterly wind stress anomalies in the western basin (Figure 2c). The reflected Kelvin wave signal is not visible in the total sea level field until August–September, when the reflected Kelvin wave amplitude is strong and the directly wind-forced Kelvin wave of the opposite sign is weaker in comparison (Figures 3b–3d).

[14] The interaction between the boreal spring AMM and the boreal summer Niño is therefore mediated by two competing mechanisms. First, zonal wind stress anomalies along the equator associated with the AMM generate equatorial Kelvin waves during April–August. The wind-forced Kelvin waves strongly affect sea level in the eastern equatorial Atlantic. These ocean responses act to reinforce the initial anomalous sea level through feedback to the wind field. Second, zonal wind stress anomalies and associate Ekman pumping in the western basin generate equatorial Rossby waves centered near 4°N. The wind-forced Rossby waves reflect off the western boundary during May–August and provide a negative feedback on the directly wind-forced equatorial anomalies in the eastern basin. The net effect of the AMM on equatorial sea level in boreal spring and summer therefore depends on the relative strengths of the forced and reflected Kelvin waves. Since sea level, thermocline depth, and SST are closely linked in the eastern equatorial Atlantic through the Bjerknes feedback, it is anticipated that the strength and timing of Atlantic Niño events may be affected by the state of the AMM during the previous spring. Further studies are needed to explore this potential link and to quantify the strengths of the positive and delayed negative feedbacks of the AMM onto the Atlantic Niño.

4. Summary and Discussion

[15] Interactions between the Atlantic meridional and Niño modes were investigated using observations and a quasi-analytical linear equatorial wave model. It was found that anomalous equatorial winds associated with the boreal spring meridional mode generate equatorial Kelvin waves that act to reinforce the initial equatorial sea level anomalies in the eastern basin during boreal spring and summer. Anomalous winds in the central and western equatorial Atlantic during boreal spring associated with the meridional mode generate equatorial Rossby waves centered near 4°N. The Rossby waves propagate westward, reflect off the western boundary during May–August, and propagate eastward along the equator as Kelvin waves. The sea level anomalies associated with the wind-forced Rossby and reflected Kelvin waves are opposite in sign to the directly wind-forced equatorial Kelvin waves. The reflected Kelvin waves therefore provide a negative feedback on the development of the Niño mode in the eastern equatorial Atlantic during May–July. A similar delayed negative feedback operates during ENSO events in the equatorial Pacific [*Battisti and Hirst*, 1989; *McPhaden and Yu*, 1999], though there first baroclinic mode waves dominate vis-à-vis the second baroclinic mode waves as in our results.

[16] These results agree with previous studies that show the importance of equatorial Kelvin waves for the development of eastern equatorial Atlantic SST anomalies [*Servain et al.*, 1982; *Hormann and Brandt*, 2009]. Our results also support the conclusion of *Servain et al.* [1999] that the meridional and Niño modes are linked through anomalous changes in equatorial winds. In addition to the positive reinforcement between the anomalous meridional

SST gradient, zonal equatorial winds, and eastern equatorial SSTs, we found a delayed negative feedback associated with wind-generated equatorial Rossby waves and their western boundary reflection.

[17] **Acknowledgments.** This work was supported by NOAA's Climate Program Office and the Joint Institute for the Study of the Atmosphere and Ocean at the University of Washington. PMEL publication 3554. JISAO contribution 1824.

References

Battisti, D. S., and A. C. Hirst (1989), Interannual variability in a tropical atmosphere-ocean model: Influence of the basic state, ocean geometry and nonlinearity, *J. Atmos. Sci.*, *46*, 1687–1712.

Carton, J. A., and B. H. Huang (1994), Warm events in the tropical Atlantic, *J. Phys. Oceanogr.*, *24*, 888–903.

Carton, J. A., X. H. Cao, B. S. Giese, and A. M. daSilva (1996), Decadal and interannual SST variability in the tropical Atlantic Ocean, *J. Phys. Oceanogr.*, *26*, 1165–1175.

Chang, P., R. Saravanan, L. Ji, and G. C. Hegerl (2000), The effect of local sea surface temperatures on atmospheric circulation over the tropical Atlantic sector, *J. Clim.*, *13*, 2195–2216.

Hormann, V., and P. Brandt (2009), Upper equatorial Atlantic variability during 2002 and 2005 associated with equatorial Kelvin waves, *J. Geophys. Res.*, *114*, C03007, doi:10.1029/2008JC005101.

Hu, Z. Z., and B. H. Huang (2006), Physical processes associated with the tropical Atlantic SST meridional gradient, *J. Clim.*, *19*, 5500–5518.

Illig, S., B. Dewitte, N. Ayoub, Y. du Penhoat, G. Reverdin, P. De Mey, F. Bonjean, and G. S. E. Lagerloef (2004), Interannual long equatorial waves in the tropical Atlantic from a high-resolution ocean general circulation model experiment in 1981–2000, *J. Geophys. Res.*, *109*, C02022, doi:10.1029/2003JC001771.

Kalnay, E., et al. (1996), The NCEP/NCAR 40-year reanalysis project, *Bull. Am. Meteorol. Soc.*, *77*, 437–471.

Keenlyside, N. S., and M. Latif (2007), Understanding equatorial Atlantic interannual variability, *J. Clim.*, *20*, 131–142.

McCalpin, J. D. (1987), A note on the reflection of low-frequency equatorial Rossby waves from realistic western boundaries, *J. Phys. Oceanogr.*, *17*, 1944–1949.

McPhaden, M. J., and X. Yu (1999), Equatorial waves and the 1997–98 El Niño, *Geophys. Res. Lett.*, *26*, 2961–2964.

Nobre, C., and J. Shukla (1996), Variation of sea surface temperature, wind stress, and rainfall over the tropical Atlantic and South America, *J. Clim.*, *9*, 2464–2479.

Reynolds, R. W., N. A. Rayner, T. M. Smith, D. C. Stokes, and W. Q. Wang (2002), An improved in situ and satellite SST analysis for climate, *J. Clim.*, *15*, 1609–1625.

Servain, J., J. Picaut, and J. Merle (1982), Evidence of remote forcing in the equatorial Atlantic Ocean, *J. Phys. Oceanogr.*, *12*, 457–463.

Servain, J., I. Wainer, J. P. McCreary, and A. Dessier (1999), Relationship between the equatorial and meridional modes of climate variability in the tropical Atlantic, *Geophys. Res. Lett.*, *26*, 458–488.

Yu, X., and M. J. McPhaden (1999), Seasonal variability in the equatorial Pacific, *J. Phys. Oceanogr.*, *29*, 925–947.

Zebiak, S. E. (1993), Air-sea interaction in the equatorial Atlantic region, *J. Clim.*, *6*, 1567–1586.

G. R. Foltz, Joint Institute for the Study of the Atmosphere and Ocean, University of Washington, 7600 Sand Point Way NE, Seattle, WA 98115, USA. (gregory.foltz@noaa.gov)

M. J. McPhaden, Pacific Marine Environmental Laboratory, NOAA, 7600 Sand Point Way NE, Seattle, WA 98115, USA.